Nanoporous Anodized Aluminum Thickness Optimization Through Pulse Current Mode

Iman Mohammadi*, Abdollah Afshar, Shahab Ahmadi

Department of Materials Science and Engineering, Sharif University of Technology, Azadi Ave; P.O. Box 11155–9466, Tehran, Iran

ARTICLE INFO

Article history:

Received 25 August 2015
Accepted 18 September 2015
Available online 20 January 2015

Keywords:

Nanoporous anodized aluminum
Pulse current
Corrosion behavior
DOE.

ABSTRACT

The purpose of this study was to optimize the thickness of anodizing Aluminum coatings processed under pulse current mode through Design of Experiments (DOE) method. Thickness measurement, polarization and electrochemical impedance spectroscopy were employed to take thickness and corrosion behaviors of the anodized coatings into consideration. Also, field-emission scanning electron microscopy (FE-SEM) was utilized to characterize the surface morphology of the coatings. It was found that thickness of the anodized coatings strongly depends on various parameters among which time, temperature and pulse current parameters (like current density limit, frequency and duty cycle) were considered in the present study. Analysis of variance (ANOVA) was used for estimating the coating thickness. Experimental results showed the maximum value for coating thickness was 62 μm being attained at the maximum and minimum current density of 6.28 and 1.55 A/dm^2, a frequency of 150.5 Hz, time of 51 min, duty cycle of 81.5% and the bath temperature of 13.5^{o}C. Also, FE-SEM observations of the surface of anodized coatings showed that this optimum condition leads to a lower porosity amount. Polarization measurements showed that this lower porosity amount causes an increase in corrosion resistance of the anodized coatings.

1. Introduction

High strength-to-weight ratio and low density of aluminum and its alloys lead to preponderant use of this alloy for a wide range of applications. However, some shortcomings of these alloys such as low hardness, poor corrosion behavior and low wear resistance have limited its application [1]. However, when these alloys are exposed to medium atmosphere, an oxide layer begins to form on aluminum surfaces. In spite of its low thickness, this oxide film improves corrosion resistance and mechanical properties of the constituents. Anodized Aluminum Oxidation (AAO) is a popular method often used to increase the thickness of this coating [1, 2].

Various investigations have dealt with the improvement of anodized coating properties by changing process parameter, among which alteration of current mode is an attractive field [3-5]. Among traditional anodizing processes, the direct current mode was typically employed in producing oxide layers. However, this method causes large heat content and leads to using lower temperature during the process [6-7]. The main drawback of these methods is a lower growth rate and cost considerations. In recent years, pulse anodizing was investigated in various studies [8-10], but hybrid pulse

* Corresponding Author:
E-mail Address: imanmohammadi68@gmail.com

anodizing as a new approach in this field leads to performing coating in an ambient temperature and decreasing imperfection of low temperature [11-13].

Lee et al. [8] suggested that pulse anodizing may improve the hardness and corrosion properties of the coatings. When using pulse method, cell accumulation and the structure of the anodized coatings are enhanced [14]. On the other hand, when using this method, heat content generated in higher current densities is dissipated on the surface of the coatings. It allows us to use a greater current density and higher electrolyte temperature in the anodizing process without burning of the coating [15-16]. Therefore, among the main advantages of pulse current one can refer to the enhancement of the corrosion resistance of the anodic layer, the considerable improvement of the efficiency of the film formation process, and the increase in thickness and surface density of the anodized coatings [11, 16]. In this regard, hybrid pulse anodizing is a new approach that leads to the performance of the coating in an ambient temperature and decreases the imperfection of low temperature [11-12].

Bensaleh et al. studied the effect of sulphuric acid anodizing conditions on the growth rate and density of anodic oxide layers using Doehlert experimental design [17]. In another research, they optimized the physical and mechanical properties of anodized films in mixed oxalic acid–sulphuric acid electrolyte by using Doehlert experimental design [18]. However, there has been no comprehensive study on the use of design of experiment (DOE) for optimizing pulse anodizing process.

As previously mentioned, the properties of the coatings are a strong function of pulse current parameters. Therefore, due to various process parameters such as pulse current, optimization of these parameters is required. The traditional optimization process uses changing one factor while keeping the other terms constant. But these methods involve a large number of tests and ignore the interactions between factors. Recently, various methods were employed for optimal among which Design of Experiment (DOE) is the most popular one [17-19]. In this study, Response Surface Methodology (RSM) based on a Central Composite Design (CCD) was used for optimizing pulse anodizing process.

2. Experimental procedures

2.1. Materials and pretreatment

The starting material for substrate in the present study was commercial pure aluminum sheet (Al 1050) with 30×20×1 mm^3 dimensions. The normal composition of this alloy was: 0.37wt.% Si, 0.001wt.% Cu, 0.26wt.% Fe, 0.001wt.% Mn, 0.047wt.% Mg, 0.01wt.% Zn and balance of Al. This material was utilized as a substrate and polished by being mechanically ground to a P1200 grade paper in order to obtain a smooth surface. Prior to anodizing, the samples were treated in the following sequence: a) The sample was degreased by ultra-sonication in acetone for 10 min, b) the sample was electropolished in a mixture of $HClO_4$ and ethanol with the volume ratio of 1:4 at 20 V for 30s at room temperature, and c) the samples were rinsed immediately with distilled water and then dried.

2.2. The anodizing process

The chemical composition of the electrolyte used for anodizing sample is shown in Table 1. A Direct Current plus Pulse (DCP) was employed to anodize the substrates. In this current mode, the four following parameters were designated to vary independently: maximum current density (I_{max}), minimum current density (I_{min}), t_{on} and t_{off}. Fig. 1 shows the relationships between the stated parameters. It is generally agreed that in pulse current, frequency and duty cycle abide by the equations (D) = 1/ (t_{on} + t_{off}) and (C) = t_{on}/ (t_{on} + t_{off}), respectively. A pulse rectifier (SL 2/25 PCS, Iran) benefiting a two–electrode method in which the sample is selected as an anode and an Aluminum sheet as cathode larger than the sample was used to produce pulse waveform.

Table 1. The chemical composition of the anodizing electrolyte

Composition	Content
H_2SO_4	g/L200
$H_2C_2O_4$	g/L20
$C_7H_6O_6S.{}_2H_2O$	10 g/L
C_3H_8O	ml/L10
$Al_2(SO_4)_3$	g/L3

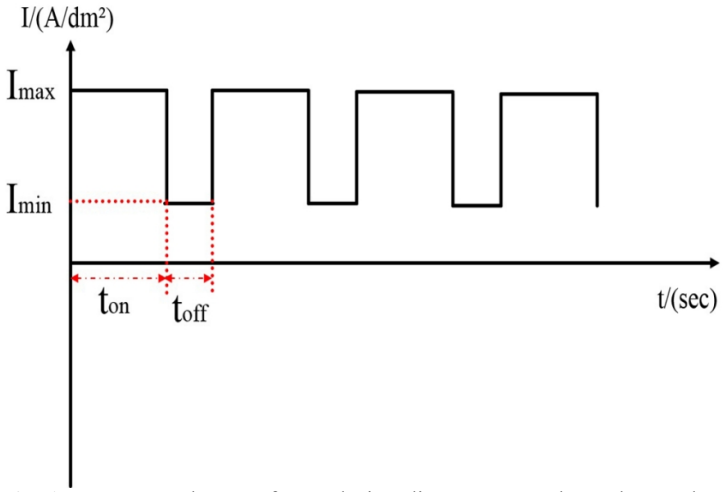

Fig. 1. Power supply waveforms during direct current plus pulse mode.

2.3. Design of Experiments methodology

Design of Experiments (DOE) was performed by Design Expert 7 software. This method was used for exploring the possible effects of the pulse parameters, i.e. maximum current density, minimum current density, duty cycle and frequency, time, temperature, and their interactions with the thickness of the anodized coatings. In order to optimize the thickness of the coatings, the Central Composition Design (CCD) method was used. In conformity with literature, the parameter ranges for optimizing are shown in Table 2.

Table 2. Process parameter range of pulse anodizing for optimizing

Parameter	Imax (A/dm^2)	Imin (A/dm^2)	Duty cycle (%)	Frequency (Hz)	Temperature (°C)	Time (min)
Range	3-7	0-3	30-95	2.5-400	10-30	10-60

According to these parameter ranges, experimental design for anodizing aluminum specimens in pulse current mode and an ambient temperature is illustrated in Table 3. As can be seen, 52 experiment procedures under various parameters conditions were designed by the CCD method. This experimental procedure involves some important details. It is implicitly understood that the standard order is not equal to the run of an experiment due to the randomization of parameters in this method. Randomization guarantees a considerable reduction in the unpleasant effects of noise and unwanted parameters on the effective factor. Also, it can be seen that the 45^{th} to 52^{th} experiments bear the same experimental range. This similarity is adopted by the software to calculate the reliability and the amount of error in the result [20]. In order to obtain maximum thickness of the anodized coatings, the parameter was optimized based on finding the best model and analysis of this model by contour and surface plot.

Table 3. Experimental design for optimizing the anodized coating under pulse current

Standard order	Run order	Imax (A/dm^2)	Imin (A/dm^2)	Duty cycle (%)	Frequency (Hz)	Temperature (°C)	Time (min)
1	11	3.7	0.5	33.5	74.3	13.6	19.0
2	17	6.3	0.5	33.5	74.3	13.6	51.0
3	46	3.7	2.5	33.5	74.3	13.6	51.0
4	31	6.3	2.5	33.5	74.3	13.6	19.0
5	45	3.7	0.5	81.5	74.3	13.6	51.0

Standard order	Run order	Imax (A/dm^2)	Imin (A/dm^2)	Duty cycle (%)	Frequency (Hz)	Temperature (°C)	Time (min)
6	35	6.3	0.5	81.5	74.3	13.6	19.0
7	1	3.7	2.5	81.5	74.3	13.6	19.0
8	37	6.3	2.5	81.5	74.3	13.6	51.0
9	20	3.7	0.5	33.5	328.2	13.6	51.0
10	52	6.3	0.5	33.5	328.2	13.6	19.0
11	13	3.7	2.5	33.5	328.2	13.6	19.0
12	43	6.3	2.5	33.5	328.2	13.6	51.0
13	28	3.7	0.5	81.5	328.2	13.6	19.0
14	12	6.3	0.5	81.5	328.2	13.6	51.0
15	41	3.7	2.5	81.5	328.2	13.6	51.0
16	27	6.3	2.5	81.5	328.2	13.6	19.0
17	33	3.7	0.5	33.5	74.3	26.4	51.0
18	40	6.3	0.5	33.5	74.3	26.4	19.0
19	25	3.7	2.5	33.5	74.3	26.4	19.0
20	38	6.3	2.5	33.5	74.3	26.4	51.0
21	2	3.7	0.5	81.5	74.3	26.4	19.0
22	47	6.3	0.5	81.5	74.3	26.4	51.0
23	39	3.7	2.5	81.5	74.3	26.4	51.0
24	42	6.3	2.5	81.5	74.3	26.4	19.0
25	21	3.7	0.5	33.5	328.2	26.4	19.0
26	51	6.3	0.5	33.5	328.2	26.4	51.0
27	48	3.7	2.5	33.5	328.2	26.4	51.0
28	18	6.3	2.5	33.5	328.2	26.4	19.0
29	32	3.7	0.5	81.5	328.2	26.4	51.0
30	10	6.3	0.5	81.5	328.2	26.4	19.0
31	14	3.7	2.5	81.5	328.2	26.4	19.0
32	16	6.3	2.5	81.5	328.2	26.4	51.0
33	30	3.0	1.5	57.5	201.3	20.0	35.0
34	8	7.0	1.5	57.5	201.3	20.0	35.0
35	44	5.0	0.0	57.5	201.3	20.0	35.0
36	4	5.0	3.0	57.5	201.3	20.0	35.0
37	15	5.0	1.5	20.0	201.3	20.0	35.0
38	26	5.0	1.5	95.0	201.3	20.0	35.0
39	19	5.0	1.5	57.5	2.5	20.0	35.0
40	49	5.0	1.5	57.5	400.0	20.0	35.0
41	7	5.0	1.5	57.5	201.3	10.0	35.0
42	29	5.0	1.5	57.5	201.3	30.0	35.0
43	50	5.0	1.5	57.5	201.3	20.0	10.0
44	9	5.0	1.5	57.5	201.3	20.0	60.0
45	36	5.0	1.5	57.5	201.3	20.0	35.0
46	23	5.0	1.5	57.5	201.3	20.0	35.0
47	3	5.0	1.5	57.5	201.3	20.0	35.0
48	6	5.0	1.5	57.5	201.3	20.0	35.0
49	24	5.0	1.5	57.5	201.3	20.0	35.0
50	5	5.0	1.5	57.5	201.3	20.0	35.0
51	22	5.0	1.5	57.5	201.3	20.0	35.0
52	34	5.0	1.5	57.5	201.3	20.0	35.0

2.4. Characterization of coatings

2.4.1. Thickness measurements

Thickness of the anodic oxide films was measured by thickness gauge with an eddy current probe (Dual Scope MP40, Germany). The measurements were taken in ten distinct points distributing uniformly on the surface of the anodized coating and an average value was reported.

2.4.2. Surface morphology

The surface morphology of the oxide layers was characterized by a Joel JSM-7000F FE-SEM.

2.4.3. Electrochemical measurements

Electrochemical measurements on the surface of oxide layers were performed using a potentiostat/galvanostat (Autolab model 302N). A three-electrode cell consisting of 3.5wt% NaCl solution at room temperature was used. In this method, the specimen was selected as the working electrode, Saturated Calomel Electrode (SCE) as the reference electrode and a graphite rod as the counter–electrode. In order to measure potentiodynamic polarization for the specimens, a scan rate of $1mVs^{-1}$ starting at -800 mV below the Open Circuit Potential (OCP) and finishing at 1V above of the OCP was employed. Electrochemical impedance spectroscopy (EIS) on the surface of oxide layers was carried out by EG&G (model 273A) under conditions analogous to potentiodynamic polarization measurement. The measurements were taken in the frequency range of 10^{-2}-10^{5} Hz with an amplitude of 10mV and the results were fitted using the ZSimpWin V3.40 software. Additionally, prior to the beginning of each test, the samples were immersed for 30 min in the solutions to establish the open circuit potential.

3. Results and discussion

In order to analyze the results of the experimental design, Analyses of Variance (ANOVA) were used the results of which are shown in Table 4. In order to predict the best model, Fisher's test (F test) was employed in which the appropriate F value and low P value were the acceptable model for predicting thickness of anodized coating [21]. As can be seen, ANOVA predicts that Quadratic model was the appropriate model due to a lower F value in this model, although the P values are the same for linear, two factorial interaction and Quadratic models. According to the results, ANOVA predicts the thickness of the coatings under maximum current density (A), minimum Current density (B), duty cycle (C), frequency (D), bath temperature (E) and anodizing time (F) as follows:

$$\text{Thickness } (\mu m) = 34.98 + 3.76A + 2.43B + 4.58C - 1.18D - 3.18E + 13.54F - 3.53A\times E - 1.9C\times E + 2.76C\times F - 3.42E\times F + 2.05A^2 - 2.7B^2 - 0.93C^2 - 3.5D^2 - 1.87E^2 - 0.58F^2 \quad (1)$$

Table 4. ANOVA result in various models which predict the thickness of the anodized coatings

Source	Sum of squares	DF	Mean square	FValue	PValue
Linear	2675.36	28	202.69	412.57	<0.0001
2FI	2876.56	13	221.27	271.45	<0.0001
Quadratic	1757.13	7	251.02	267.75	<0.0001
Cubic	5.72	1	5.72	95.45	0.001
Pure error	3.7	5	0.74		

Also, Normal Probability Plot (NPP) was used to evaluate the normality of the data. The results are presented in Fig. 2. As can be seen, the residuals are normally distributed along the straight line (residuals fall approximately). Residual means the variation between the observed and the predicted values [22].

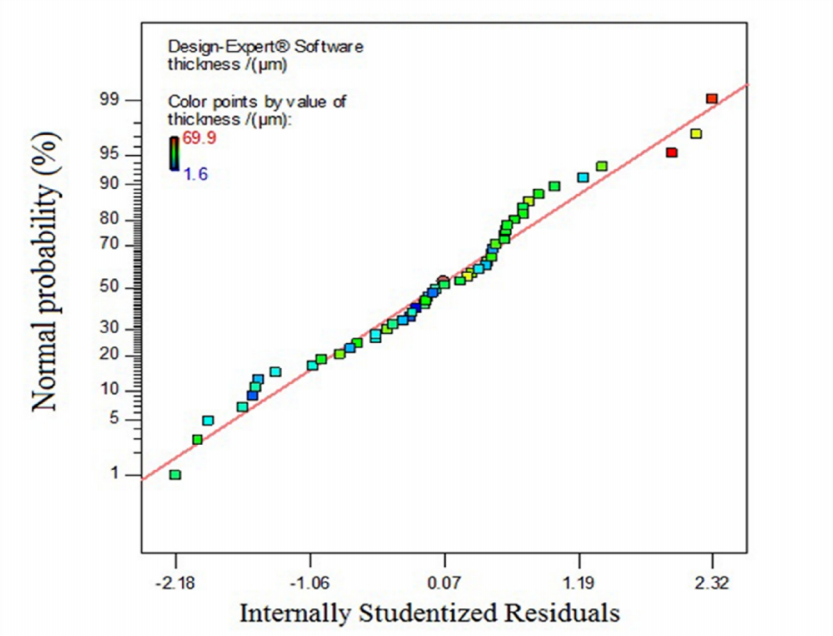

Fig. 2. Normal Probability Plot of residuals for thickness of the anodized coating under pulse current

The next purpose of this study is to optimize the maximum current density, minimum current density, frequency, duty cycle, time and temperature of the processing aiming to obtain the maximum thickness of the coatings. Hence, the coefficient of this equation and surface and contour plot (In surface and contour plots two factor variable and other parameter are constant) was used. The results indicated that unlike the frequency, time and duty cycle of anodizing are the most popular parameters affecting the thickness of the anodized coating, as reported in Eq. 1 & Fig. 3.

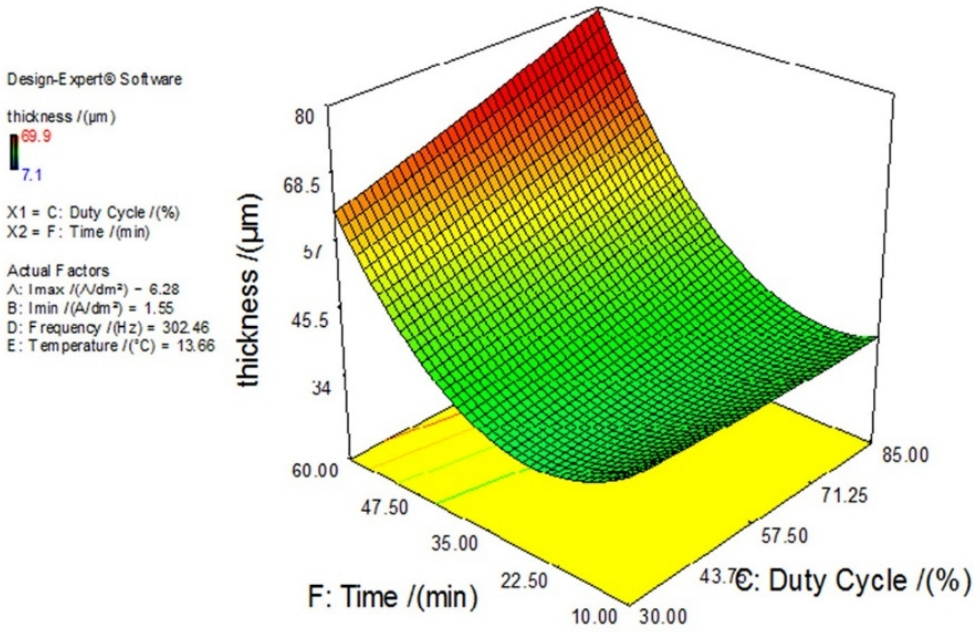

Fig. 3. Effect of duty cycle and time on the thickness of the anodized coating under pulse current

3.1. Effect of temperature on the thickness of the anodized coatings

According to Eq. 1, temperature has a negative coefficient and it is expected that undesirable influences on the thickness of coatings are produced by pulse anodizing. Decreasing the coating thickness is attributed to the notion that the formation of anodized coatings is determined based on a fierce competition between growth and dissolution speed generated by the electrolyte. The Al_2O_3 coating is formed by transmission of the Al^{3+} ion from the substrate and O^{2-} from the solution to the coating in the opposite direction through the interface of metal/anodic film/electrolyte [1]. When the electrolyte temperature begins to increase, aggressiveness of the electrolyte increases [23-24] and decreases the thickness of the coatings.

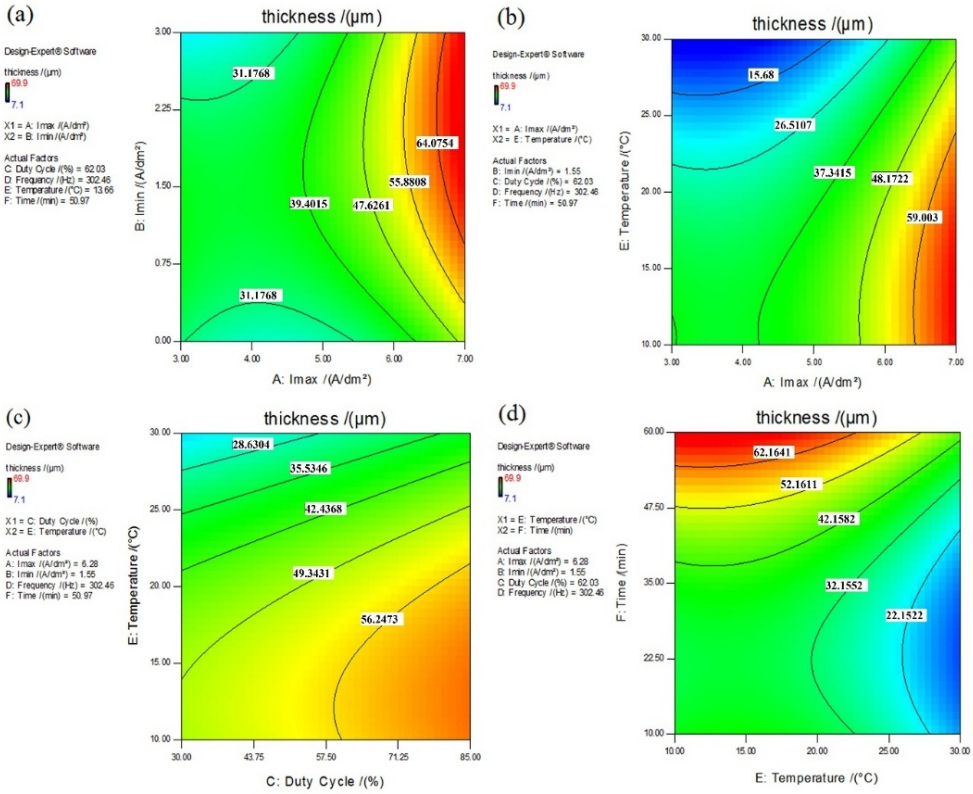

Fig. 4. Contour plots for studying the thickness of anodized coating under various condition: (a) maximum and minimum current density, (b) maximum current density and temperature, (c) duty cycle and temperature and (d) time and temperature

3.2. Effect of current density on the thickness of the anodized coatings

According to Eq. 1, coefficients of maximum current density and minimum current density bear positive values and by increasing these parameters, thickness of the coatings begins to increase, as shown in Fig. 4a. It is due to this fact that according to Faraday's law, thickness of the coatings is proportional to the current density and anodizing time [10]. So, with an increase in current density, thickness of the coating increases. On the other hand, with an increase in current density, the formation of Al_2O_3 on the surface of the coating is encouraged. As this chemical reaction is an exothermic one, begins to rise temperature and other side increase in current density causes to heat on the surface of anodic layer. Therefore, dissolution speed of the anodized coatings by the electrolyte increases and overcomes the growth speed [24-25]. When the minimum current density increases, this effect comes to a critical state. It is associated with an affecting mechanism of recovery behavior of pulse

current. Increasing this parameter leads to an increase in the heat content on the surface of the anodized coating, so the coefficient B^2 has a negative value and when increasing minimum current density, this parameter overcomes the positive coefficient B and leads to a reduction in thickness of the coating. Fig. 5 shows the effect of minimum current density increment on morphology of the anodized coatings. Comparison of Fig. 5b with Fig. 5c demonstrates that applying greater average current densities leads to increase in pore diameter. Therefore, the interaction of current density with temperature has an important effect on thickness of the anodized coating, as shown in Fig. 4b.

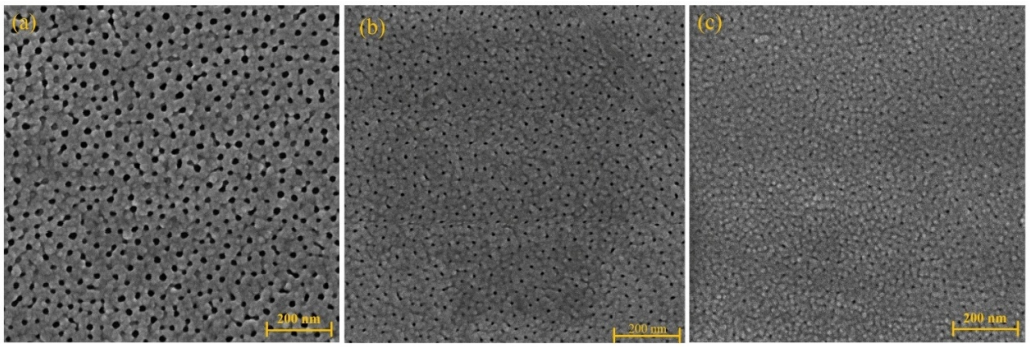

Fig. 5. FE-SEM micrographs of the surfaces anodized in the condition: (a) direct current mode by current density of $4A/dm^2$ and the bath temperature of 10^oC, (b) optimized and (b) standard order 8

3.3. Effect of duty cycle on the thickness of the anodized coatings

Duty cycle is one of the most popular parameters affecting thickness of the coatings produced under pulse current. When the duty cycle increases, anodizing of the sample is carried out by greater current density. Although, increasing current density according to Faraday's law leads to an increase in thickness of the anodized coating, when duty cycle reaches a maximum (i.e. direct current) it causes the temperature to localize on the surface of anodic layer and decrease the thickness of anodized coating (the coefficient C^2 can justify this effect). It traces back to this fact that direct current encourages the release of gas bubbles [6-7] (resulting from oxidation heat and molecule forming of oxygen atoms [24]) on the surface of the anodized layer.

Due to a significant difference between thermal conductivities of this gas and the oxide layer, the heat content on the surface concentrates and rises temperature, hence increasing the solution aggressiveness and dissolution on the surface of anodic layer and decreasing thickness of coating (Fig. 5a). Due to this effect and according to Eq. 1 and Fig. 4c, interaction of duty cycle with temperature has a negative effect on thickness of the anodized coatings.

3.4. Effect of frequency on the thickness of the anodized coatings

According to Eq. 1, frequency has no significant effect on thickness of the coatings, but when frequency increases, not only the mechanism of dissolution is stimulated in the defect structure, but also in other structures, this dissolution occurs and leads to a reduction in thickness of the coatings.

3.5. Effect of time on the thickness of the anodized coatings

Time is an important factor affecting the thickness of the anodized coatings. According to Fig. 3 and Eq. 1, with an increase in time or interaction of time and duty cycle, the thickness of the anodized coating increases. It is related to the fact that the thickness of the anodized coating is modulated by Faraday's law, and that by raising the anodizing time, thickness of anodized coating increases. Therefore, increasing duty cycle and time leads to an increase in the thickness of the coatings, but based on the coefficient F^2, increasing the anodizing time leads to a

decrease in coating thickness due to Powdery of coatings [13, 26].

Based on Eq. 1 and Fig. 4d, the coefficient for interaction of time with temperature has a negative value. It is due to this fact that when duration time increases, the effective surface of coating increases, so larger gas bubble content leads to an escalation in the heat content and temperature on the surface of the anodic layer [25]. Therefore, an increase in the anodizing time leads to increasing dissolution and decreasing the thickness of the anodized coating.

3.6. Optimal point

Table 5 illustrates the optimum point by 95% confidence for obtaining a thick layer. As can be seen, these six selected levels for the maximum current density, minimum current density, frequency, duty cycle, time and temperature will give a thickness of 62 µm. Also, results show that the confidence interval range for this prediction is 35.8–88.1 µm. For calculating the confidence of prediction point that is suggested by the software, confirmation run is evaluated in optimal point. Then, this point will be compared with the confidence intervals according to the prediction equation [20]. Results show that the thickness of the coatings in optimal point is 60.6 µm, which is not sustainably different from the predicted value. Fig. 6 shows the predicted verse actual thickness of the anodized coatings. As seen, the actual values are near to the standard line, implying that the predicted point is acceptable. In this figure, the thickness value is shown by color.

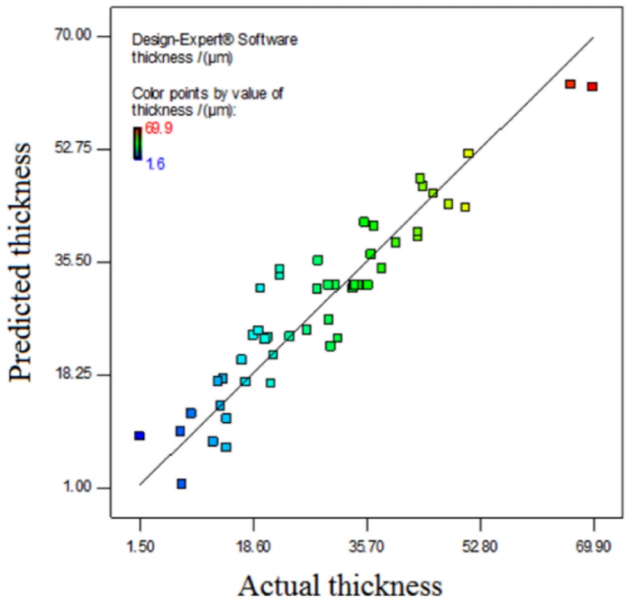

Fig. 6. Actual thickness vs. Predicted thickness of anodized coating by DOE software

Table 5. Intervals ranges for prediction point and 95% confident for obtain thick layer under pulse anodizing

Factor	Name	Level	Low level	High level
A	Imax /(A/dm²)	6.28	3.72	6.28
B	Imin /(A/dm²)	1.55	0.54	2.46
C	Duty Cycle /(%)	81.46	33.54	81.46
D	Frequency /(Hz)	150.46	74.26	208.24
E	Temperature /(°C)	13.66	13.61	26.39
F	Time /(min)	50.97	19.03	50.97
Thickness /(µm)	62.01544	24.87-99.16	35.88	88.15
Response	(Prediction)	(95% PI low and 95% PI high)	(95% CI low)	(95% CI high)

3.7. Corrosion behavior

3.7.1. Potentiodynamic polarization measurements

The potentiodynamic polarization of the specimens was measured under various conditions. For this aim, a 3.5 wt%-NaCl solution was used. In order to obtain the values of Ecorr and Icorr, Tafel slope extrapolation of the polarization curves were made. The results are shown in Fig. 7 and Table 6. As can be observed, the corrosion potential of the sample anodized under optimum conditions -598.23 mV (vs. SCE) is much more than that processed under DC current mode, -828.6 mV (vs. SCE) mV (vs. SCE) and the results show that the corrosion current density of this coating is reduced from 1132 to 1.9 nA/cm^2 for the DC current mode and the optimized specimens, respectively. It is due to larger surface density of the coating in optimum sample, as observed in Fig. 5. Equation (2) is applied in order to calculate the polarization resistances.

$$1/R_P = 2.303 \frac{\beta_a + \beta_c}{\beta_a \beta_c} i_{corr} \quad (2)$$

Where RP is polarization resistance, βa and βc are anodic β and cathodic β, respectively.

Table 6. Electrochemical parameters of the samples anodized under conditions of optimized, standard order 8 and direct current mode by current density of 4A/dm^2 and the bath temperature of 10°C

specimen	Polarization parameters			EIS parameters		
	Icorr (nA/cm^2)	Ecorr (mV vs SCE)	Rp (KΩ/cm^2)	n	CPE$_{barr}$ (μF/cm^{2}s^n)	R$_{barr}$ (Ω cm^2)
Optimized	1.9	-598.23	6055	0.954	8.01	4.5×10^6
Standard order 8	41.39	-698.61	283.63	0.885	31.2	9.8×10^5
DC current mode	1132	-828.6	1.46	0.65	52.1	3.8×10^5

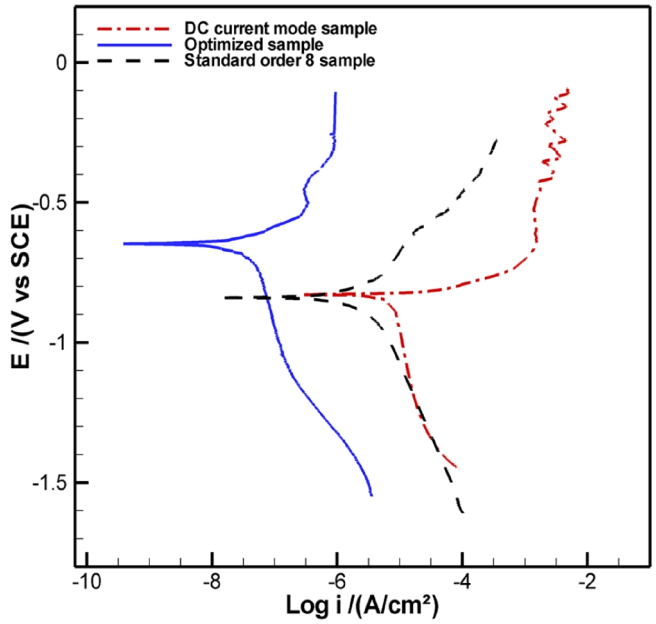

Fig. 7. Polarization curves for the samples that anodized in the condition of optimized, standard order 8 and direct current mode by current density of 4A/dm^2 and the bath temperature of 10°C

The corrosion properties of the anodized coatings are firstly affected by pore diameter. The result is implicitly derived from Fig. 7. In fact, when the sample is

anodized under DC current mode, localized heat content is concentrated on the surface of the anodic film, leading to an increase in dissolution rate, pore diameter, defects and voids on the anodic film analogous to what was mentioned in the previous section. Thus, according to Fig. 5a, when DC current mode is used, the surface density begins to decrease more than what occurs in the pulse current mode, thereby reducing the corrosion properties of the samples.

3.7.2. Electrochemical impedance spectroscopy

In order to confirm the obtained data from Potentiodynamic polarization, EIS study was performed. Fig. 8 presents the Nyquist and Bode plots for differently processed coatings. Equivalent circuit assignation over collected data was done by ZSimpWin V3.40 software. The impedance data were analyzed using the simplified equivalent circuit of Fig. 9, as widely proposed in the literature [13, 25, 27]. In the case of this structure, there exist two constant phase elements (CPE) as follows:

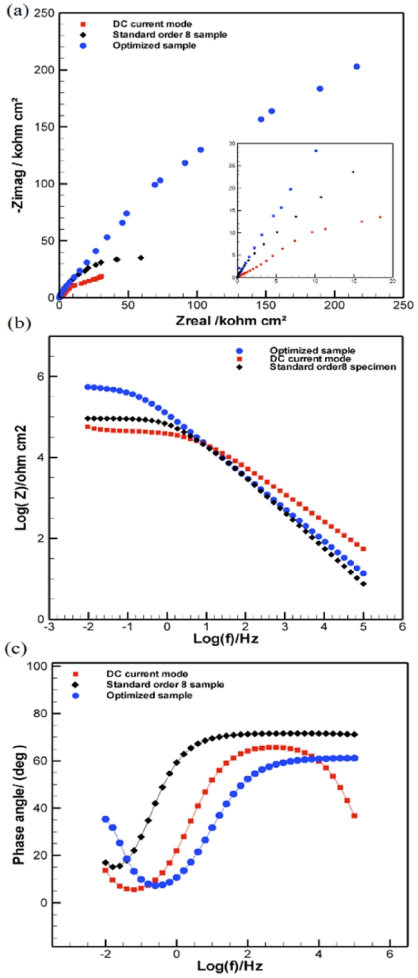

Fig. 8. (a) Nyquist plots, (b) Bode and (c) Bode-phase plots of the samples anodized under conditions of optimized, standard order 8 and direct current mode by current density of 4A/dm^2 and the bath temperature of 10°C

(i) CPE_{wall} that is associated with the capacitive behavior of the porous oxide structure.

(ii) CPE_{barr} which describes the behavior of the barrier layer. This parameter is believed to

show non-ideal capacitive behavior in both CPE.

Other components R_{sol}, R_{wall} and R_{barr} present resistive behavior of the solution, of the solution in the pore structure and of the barrier layer.

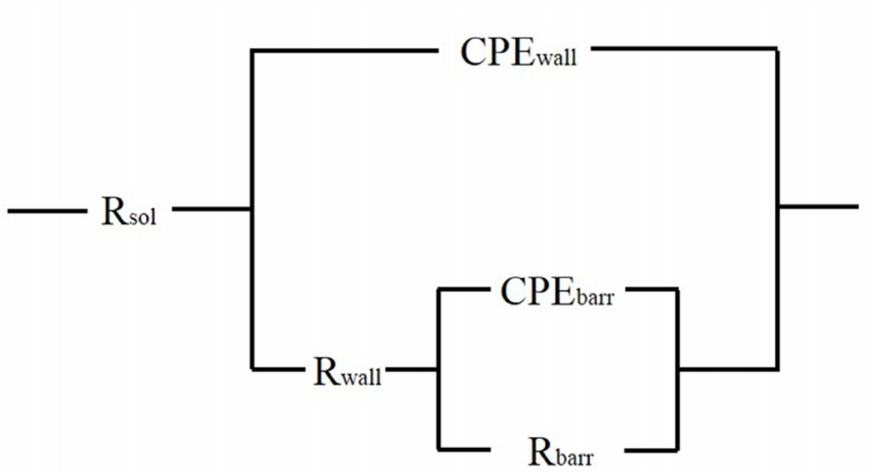

Fig. 9. Equivalent electronic circuit for coating with a double structure of porous and barrier layer

Drawing a quantitative comparison between polarization data and the results pertinent to the Nyquist plots shows a similar behavior. It is ascribed to the formation of the AAO layer with a macroscopically similar characteristic of the surface of the sample.

As can be seen, the trend of these diagrams is similar for all samples. Also, the capacitance loop diameter (Fig. 8a) and Z modulus (Fig. 8b) of the sample anodized under optimized condition is substantially greater than that of the sample anodized in DC current mode. It is found that the impedance resistance of the AAO film processed in pulse current mode decreases following a change in the optimum condition.

The lower polarization resistance (R_p) in the sample that was anodized in DC current mode could also be discussed by means of the parameter n. The value of n corresponds to the linear slope modulus of bode plot (Fig. 8b), and it is well known that when n is near 1, the surface is uniform and smooth. On the other hand, lower values (in our case n=0.65 in the specimen that was anodized in DC current mode) shows deviation from ideal capacitive behavior (which has been attributed to the inhomogeneity of the surface) and deterioration in corrosion resistance [26]. As seen in Table 6, compared to the optimum sample, the DC specimen has a lower n value. It is due to the fact that increasing dissolution on the surface of the anodic layer can lead to an increase in defect in structure. Also, in the optimum condition, the coating dissolution was controlled in order to obtain a thick layer and decrease in dissolution leads to a greater surface density. Hence, the greater corrosion resistance of the anodized coating is obtained during anodizing the sample under optimum conditions.

4. Conclusion

In this investigation, design of experiment method was used based on the central composite design for studying the possible effect of maximum current density, minimum current density, frequency, duty cycle, time and temperature on the thickness of anodized coatings. It was found that the maximum thickness of the coatings was 62 μm being attained at the maximum and minimum current densities of 6.28, 1.55 A/dm^2, a frequency of 150.5 Hz, time of 51 min, duty cycle of 81.5% and the bath temperature of 13.5^{o}C. Furthermore, the results showed that optimal thickness condition can lead to higher surface density, as verified by FE-SEM image and lead to an increase in corrosion behavior of the anodized coatings. The obtained results showed that the generated temperature during the anodizing process is one of the most

important parameters affecting the thickness of the anodized coatings. On the other hand, the results showed that this temperature can be controlled by pulse anodizing parameters. Therefore, maximum thickness of the anodized coating is obtained during pulse anodizing.

References

[1] Santos, L. Vojkuvka, J. Pallarés, J. Ferré-Borrull, L.F. Marsal, "In situ electrochemical dissolution of the oxide barrier layer of porous anodic alumina fabricated by hard anodization", Electoral. Chem., vol. 632, no. 1-2, 2009, pp. 139-142.

[2] H.S. kim, D.H. Kim, W. Lee, S.H. Cho, J.H. Hahn, H.S. Ahn, "Tribological properties of nanoporous anodic aluminum oxide film", Surf. Coat. Technol, vol. 205, no. 5, 2010, pp. 1431-1437.

[3] M. Salerno, N. Patra, R. Losso, R. Cingolani, "Increased growth rate of anodic porous alumina by use of ionic liquid as electrolyte additive", Mater. Let. , vol. 63, 2009, pp. 1826-1829.

[4] W.X. Wei, D. L. Hong, "Preparation of PTFE composite anodic film on aluminium alloy 6061 using electrophoretic process", Tribol. Mater. Surf. Interface., vol. 4, 2010, pp. 74−77.

[5] M. A. Song-Jiang, L. Peng, Z. Hai-Hui, F. Chao-Peng, K.Ya-Fei, "Preparation of anodic films on 2024 aluminum alloy in boric acid-containing mixed electrolyte", Trans. Nonferrous Met. Soc. China, vol. 18, 2008, pp. 825-830.

[6] X. F. Zhu, D. D. Li, Y. Song, and Y. H. Xiao, "The study of oxygen bubbles of anodic alumina based on high purity aluminum", Mater. Let, vol. 59, 2005, pp. 3160– 3163.

[7] H. Habazaki, H. Konno, K. Shimizu, S. Nagata, P. Skeldon and G. E. Thompson, "Incorporation of transition metal ions and oxygen generation during anodizing of aluminium alloys", Corros. Sci, vol. 46, 2004, pp. 2041-2053.

[8] W. Lee, K. Schwirn, M. Steinhart, E. Pippel, R. Scholz and U. Gösele, "Structural engineering of nanoporous anodic aluminum oxide by pulse anodization of aluminium", Nat. nanotechnol., vol. 3, 2008, pp. 234-239.

[9] M. Mirzaei and M.E. Bahrololoom, "Influence of pulse currents on the nanostructure and color absorption ability of colored anodized aluminum", Vacuum, vol.99, 2014, pp. 277-283.

[10] X. Zhao, G. Wei, X. Meng, A. Zhang, "High performance alumina films prepared by direct current plus pulse anodisation", Surf. Eng., vol. 30, 2014, pp. 455-459.

[11] C. K. Chung, R. X. Zhou, T. Y. Liu, W. T. Chang, "Hybrid pulse anodization for the fabrication of porous anodic alumina films from commercial purity (99%) aluminum at room temperature", Nanotechnol., vol. 20, 2009, pp. 055301-55305.

[12] C.K. Chung, W.T. Chang, M.W. Liao, H.C. Chang, "Effect of pulse voltage and aluminum purity on the characteristics of anodic aluminum oxide using hybrid pulse anodization at room", Thin. Solid. Film. , vol. 519, 2011, pp. 4754-4758.

[13] I. Mohammadi, A. Afshar, "Modification of nanostructured anodized aluminum coatings by pulse current mode", Surf. Coat. Technol., vol. 278, 2015, pp. 48-55.

[14] H. H. Shih and S. L. Tzou, Study of anodic oxidation of aluminum in mixed acid using a pulsed current", Surf. Coat. Technol., vol. 124, 2000, pp. 278–285.

[15] W. Wu, J. S. Yuan, S. H. Kang, A.S. Oates, Electromigration subjected to Joule heating under pulsed DC stress, Solid-state. Electron., vol. 45, 2001, pp. 2051–2056.

[16] L. E. Fratila-Apachitei, J. Duszczyk, L. Katgerman, A1−Si−(Cu) anodic oxide layers formed in H2SO4 at low temperature using different current waveforms", Surf. Coat. Technol., vol. 165, 2003, pp. 232−240.

[17] W. Bensalah, M. Feki, M. Wery and H.F. Ayedi, "Thick and Dense Anodic Oxide Layers Formed on Aluminum in Sulphuric Acid Bath", Mater. Sci. Technol., vol. 26, no. 2, 2010, pp.113-118.

[18] W. Bensalaha, K. Elleuch, M. Feki, M. Depetris-Wery and H.F. Ayedi, "Optimization of tartaric/sulphuric acid anodizing process using Doehlert design", Surf. Coat. Technol., vol. 207, 2012, pp. 123–129.

[19] I. Imanieh, E. Yousefi, A. Dolati and M.R. Mohammadi, "Experiments Design for

Hardness Optimization of the Ni-Cr Alloy Electrodeposited by Pulse Plating", Acta Metall. Sin. (Engl. Let.), vol. 26, no. 5, 2013, pp. 558–564.

[20] R.G. Brereton, "Applied Chemometrics for Scientists", John Wiley & Sons, Ltd, UK, 2007.

[21] E.R. Rene, M.S. Jo, S.H. Kim and H.S. Park, "Statistical analysis of main and interaction effects during the removal of BTEX mixtures in batch conditions, using wastewater treatment plant sludge microbes", Environ. Sci. Tech, 4 (2007) 177-182.

[22] J. Antony, "Design of Experiment for Engineers and scientists", Elsevier Science & Technology Books, New York, 2003.

[23] K. Yokohama, H. Konno, H. Takahashi and M. Nagayama, "Advantage of pulsed Anodizing", Plat. Surf. Finish. Vol. 69, 1982, pp. 62-65.

[24] W. X. Wei and C. C. Yin, "Influence of oxidation heat on hard anodic film of aluminum alloy", J. Trans. Nonfer. Met. Soc. China, vol. 22, no. 11, 2012, pp. 2707−2712.

[25] T. Aerts, J-B. Jorcin, I. D. Graeve and H. Terryn, "Comparison between the influence of applied electrode and electrolyte temperatures on porous anodizing of aluminium", Electrochem. Acta., vol. 55, 2010, pp. 3957-3965.

[26] P. Chowdhury, A.N. Thomas, M. Sharma, H.C. Barshilia, "An approach for in situ measurement of anode temperature during the growth of self-ordered nanoporous anodic alumina thin films: Influence of Joule heating on pore microstructure", Electrochim. Acta, vol. 115, 2014, pp. 657-664.

[27] M. García-Rubioa, P. Ocón, A. Climent-Font, R. W. Smith, M. Curioni, G. E. Thompson, P. Skeldon, A. Lavía and I. García, "Influence of molybdate species on the tartaric acid/sulphuric acid anodic films grown on AA2024 T3 aerospace alloy, Corros. Sci., vol. 51, no. 9, 2009, pp. 2034-2042.